RESEARCH

HOXA9 promotes proliferation, metastasis and prevents apoptosis in hepatocellular carcinoma

Guojian Bao[1,2] · Haowei Wei[1,2] · Jiawu Yan[1,2] · Yunzheng Li[1] · Cailin Xue[1] · Rao Fu[1,2] · Minglu Zhang[1,2] · Jialu Ding[2,3] · Hengqian He[4] · Decai Yu[1] · Fei Yang[2] · Beicheng Sun[1,2,3]

Abstract

Purpose This research aimed to evaluate the expression level of Homeobox A9 (HOXA9) and its role in tumorigenesis of hepatocellular carcinoma (HCC).

Methods Bioinformatic analysis, qPCR and Western blot analysis of clinical samples were employed to evaluate mRNA and protein levels of HOXA9 in HCC patients and cell lines. In vitro cell proliferation, migration and invasion, cloning formation, xenograft tumor model, wound healing and apoptosis assays, RNA sequencing analysis of RPL38-silenced HCC-LM3 cells and qPCR, Western blot analysis were performed for validation. Analysis of HOXA9-related genes were conducted to identify their relationships between HOXA9.

Results HOXA9 is dramatically upregulated in HCC. Upregulation of HOXA9 in HCC predicts poor survival of patients. Besides, HOXA9 promotes proliferation, metastasis and prevents apoptosis in HCC in vitro. In addition, HOXA9 controlled by Ribosomal protein RPL38 is upregulated in HCC. Bioinformatic analysis also indicated that HOXA9 is involved in the regulation of DNA methylation and immune infiltration in HCC.

Conclusion HOXA9 is dramatically upregulated in hepatocellular carcinoma and predicts poor prognosis. Besides, HOXA9 promoted proliferation and metastasis and prevented apoptosis in vitro, which is regulated by Ribosomal protein RPL38 in HCC.

Keywords Hepatocellular carcinoma · HOXA9 · Homeobox gene · Proliferation · Metastasis · Apoptosis

Introduction

Primary liver cancer (PLC) covered about 906,000 new cases and 830,000 deaths according to the latest data (Sung et al. 2021). In the past 20 years, with the aging and population growth, as well as the increase of age-specific incidence, new cases of liver cancer are still increasing by years (Global Burden of Disease Cancer et al. 2018; Wu et al. 2018). New cases and deaths of liver cancer could increase more than 55% by 2040 (Rumgay et al. 2022). The causes of hepatocellular carcinoma (HCC) are complex and often accompanied by cirrhosis, leading to a big challenge of HCC therapy whose ineffectiveness is also due to the high heterogeneity of HCC patients (Li and Wang 2016; Xu et al. 2019). Recently, the tumor

---

Guojian Bao, Haowei Wei, Jiawu Yan these authors contributed equally to this work.

✉ Decai Yu
yudecai@nju.edu.cn

✉ Fei Yang
fightingforever77@126.com

✉ Beicheng Sun
sunbc@nju.edu.cn

[1] Affiliated Hospital of Medical School, Nanjing Drum Tower Hospital, Nanjing University, Nanjing 210008, Jiangsu Province, China

[2] Department of Hepatobiliary Surgery, The First Affiliated Hospital of Anhui Medical University, Hefei 230022, Anhui Province, China

[3] Nanjing Drum Tower Hospital Clinical College of Nanjing University of Chinese Medicine, Nanjing 210008, Jiangsu Province, China

[4] Department of Ophthalmology, The Affiliated People's Hospital of Ningbo University, The Eye Hospital of Wenzhou Medical University (Ningbo Branch), Ningbo 315040, Zhejiang Province, China

microenvironment plays a crucial role in the development and progression of HCC, demanding for better molecular and cellular characterization of additional biomarkers to guide clinical decisions (Donne and Lujambio 2023).

Homeobox genes (*Hox*), a highly conserved group of genes in the homeobox superfamily and consisting of 39 *Hox* genes, are distributed in four clusters in mammals (Krumlauf 2018). *HoxA9*, as a member of locus A *Hox* genes, functions as either an oncogene or a suppressor gene, which makes it a challenge to conduct clinical treatment with HOXA9 inhibitors (Tang et al. 2022). Aberrant expression of HOXA9 is a prevalent feature of the most aggressive forms of acute leukemia (Collins and Hess 2016). HOXA9 inhibits the development of cutaneous squamous cell carcinoma by interacting with CRIP2 to inhibit HIF-1α-mediated glycolysis (Zhou et al. 2018). The expression of HOXA9 is down-regulated in breast cancer, which is related to the malignant degree of breast cancer by regulating BRCA1 expression (Gilbert et al. 2010). However, the expression and function of HOXA9 in HCC development haven't been totally understood.

Ribosomal protein RPL38 has been reported to be responsible for development-defective mouse mutants and lack of RPL38 results in selective downregulation in translation of several *Hox* genes essential for bone development, leading to compensatory changes in bone architecture (Kondrashov et al. 2011). Mechanically, through recognition of Internal Ribosome Entry Sites (IRES) regions in the 5'UTRs, RPL38 affects skeletal development in mice by specifically regulating the translation of multiple *Hox* genes including *HoxA9* (Xue et al. 2014). Thus, whether the regulation of *Hox* family by RPL38 is involved in the progression of HCC deserves further investigation.

In our study, in order to explore the relationship between HCC and *HoxA9*, public data available were collected and integrated. Afterwards, we validated the expression of HOXA9 in HCC clinical samples and cell lines. Then the gain-and-loss biology assay, including cell proliferation, migration and invasion, cloning formation, xenograft tumor model, wound healing and apoptosis assays were performed to discover the bio-function of HOXA9 in HCC. Moreover, we identified that the expression of HOXA9 controlled by RPL38 is upregulated in HCC. Our study provides a novel therapeutic target for HCC.

Methods and materials

HOXA9 expression analysis

Tabula Muris mouse single cell open-source datasets were obtained from GEO dataset: GSE109774.

TIMER2.0 (http://timer.cistrome.org/) were used to determine the differential expression of HOXA9 between cancers and their adjacent normal tissues with TCGA database.

The data of TCGA (The Cancer Genome Atlas) datasets were collected from the GDC (Genomic Data Commons Datga Portal) website (https://portal.gdc.cancer.gov/). The genomic information from healthy individuals was supplemented from The Genotype-Tissue Expression (GTEx) (https://www.gtexportal.org/home/).

In GEO (Gene Expression Omnibus) datasets, we mainly screened and downloaded the hepatocellular carcinoma related data collection (http://www.ncbi.nlm.nih.gov/geo/), including GSE25097, GSE36376 and GSE54236.

TCGA data analysis tool, UALCAN database (http://ual-can.path.uab.edu/analysis-prot.html) was utilized to explore the expression level of HOXA9 in LIHC among groups of patients according to different clinical parameters.

For survival analysis, the Log-Rank test was employed to compare the survival differences in different cancers from the Human Protein Atlas website (https://www.proteinatlas.org/).

Analysis of HOXA9-related expressed genes

Pearson correlation analysis was used to screen the coexpressed genes of HOXA9 in LIHC by using the LinkedOmics database (http://www.linkedomics.org/). Coexpressed genes were visualized using a volcano map, and Gene ontology (GO) analysis and Kyoto Encyclopedia of Genes and Genomes (KEGG) analysis were performed to determine the function of HOXA9. P.adj < 0.05 & q.value < 0.2 was considered statistically significant.

Immune cell infiltration analysis

The relationships between HOXA9 expression and marker genes of immune cells were explored via the TIMER database. Several algorithms, such as TIMER, EPIC, QUANTISEQ, XCELL, MCPCOUNTER, CIBERSORT, CIBERSORT-ABS, and TIDE, were applied to explore the correlation. Positive correlation (0–1) are indicated with the red color, while negative correlation (−1 to 0) are indicated with the blue color; $P < 0.05$ is considered as statistically significant.

DNA methylation analysis

TCGA data analysis tool, UALCAN database (http://ualcan.path.uab.edu/analysis-prot.html) was utilized to explore the expression of the promoter methylation level of HOXA9 in LIHC among groups of patients according to different clinical parameters.

Tissue samples

HCC specimens and adjacent tissues were randomly selected from The First Affiliated Hospital of Anhui Medical University. All patients were provided with written informed consent. In the study, all experimental procedures were approved by the Ethics Committee of The First Affiliated Hospital of Anhui Medical University and conformed to the requirements of the Declaration of Helsinki and the International Ethical Guidelines for Biomedical Research Involving Human Subjects.

RNA sequencing analysis

RNA samples for sequencing were collected, quantified, and purified from RPL38-silenced HCC-LM3 cells and parental cells. Experts from Lc-Bio Technology (Hangzhou) constructed the sequence library and performed the whole experimental process.

Cell culture

Human normal liver cell line THLE-2, hepatocellular carcinoma cell lines Hep3B, HepG2 and Huh7 were purchased from cell bank Shanghai branch, Chinese Academy of Sciences, China (Shanghai, China). HCC-LM3 and MHCC-97H were purchased from the Liver Cancer Institute, Zhongshan Hospital, Fudan University (Shanghai, China).

CRISPR/Cas9 mediated RPL38 knockout

Rpl38 gene knockout was performed by CRISPR/Cas9 technology. On the NCBI website (http://www.ncbi.nlm.nih.gov/), we searched information of human *Rpl38* gene (ID: 6169) and sgRNA sequences targeting *Rpl38* gene were designed online (https://zlab.bio/guide-design-resources).

shRNA mediated HOXA9 knockdown

HoxA9 gene knockdown was mediated by shRNA-lentivirus technology. On the NCBI website (http://www.ncbi.nlm.nih.gov/), we searched information of human *HoxA9* gene (ID: 3205) and shRNA sequences targeting HOXA9 gene were designed (Sangon biotechnology, China). The sequences of shRNA primers were listed in Supplementary Table 1.

Quantitative real-time PCR (qRT-PCR)

Quantitative real-time PCR was performed using SYBR according to the manufacturer's instructions. Relative gene expression was calculated with the $2^{-\Delta\Delta CT}$ method and data was plotted with GraphPad Prism 8. The sequences of the primers were listed in Supplementary Table 1.

Plasmid construction

To generate Flag fusion plasmid Flag-RPL38 and Flag-HOXA9, sequences were amplified and inserted into pLVX-IRES-puro (Sangon Biotech, China) lentiviral vector and verified by DNA sequencing.

Western blot

The primary antibodies used are listed in Supplementary Table 2.

Cell proliferation assay

Cell counting kit-8 (CCK-8) (Dojindo, Japan), 5-Ethynyl-2′-deoxyuridine (EdU) (Beyotime, China) and colony formation assay were employed to measure cell proliferation. The colony assay required approximately 500 cells to be plated into 6-well plates and cultured for 2 weeks. Cells were fixed with 4% paraformaldehyde and the number of clones was counted using ImageJ (NIH, USA) after crystal violet staining.

Migration and invasion assays

Corning Costar Transwell 24-well plates (8 mM) were used to evaluate the migration and invasion ability of HCC cell lines. To perform the invasion assay, a total of 50,000 cells were inoculated into an upper cavity pre-coated with 30 μg Matrigel (BD Biosciences, USA). At the indicated time, the upper cavity were removed and the cells were fixed with methanol and stained with crystal violet.

Cell apoptosis assay

The cells were resuspended in 200 μL Binding Buffer with 10 μL Annexin V-FITC and 10 μL PI solution at room temperature in darkness for 15 min after which 300 μL Binding Buffer was mixed into the resuspension. Flow cytometry was used to detect cell apoptosis within one hour.

Wound-healing assay

For wound healing assays, after the cells are fused up to 90%, a scratch is made with a 10 μL plastic pipette tip. The scratches were photographed at 0 and 48 hours after injury and analyzed by ImageJ software.

Immunohistochemical assay

The tissue sections were stained with indicated antibody and photographed with a microscope. The scores of HOXA9 protein levels were determined by multiplying the positive
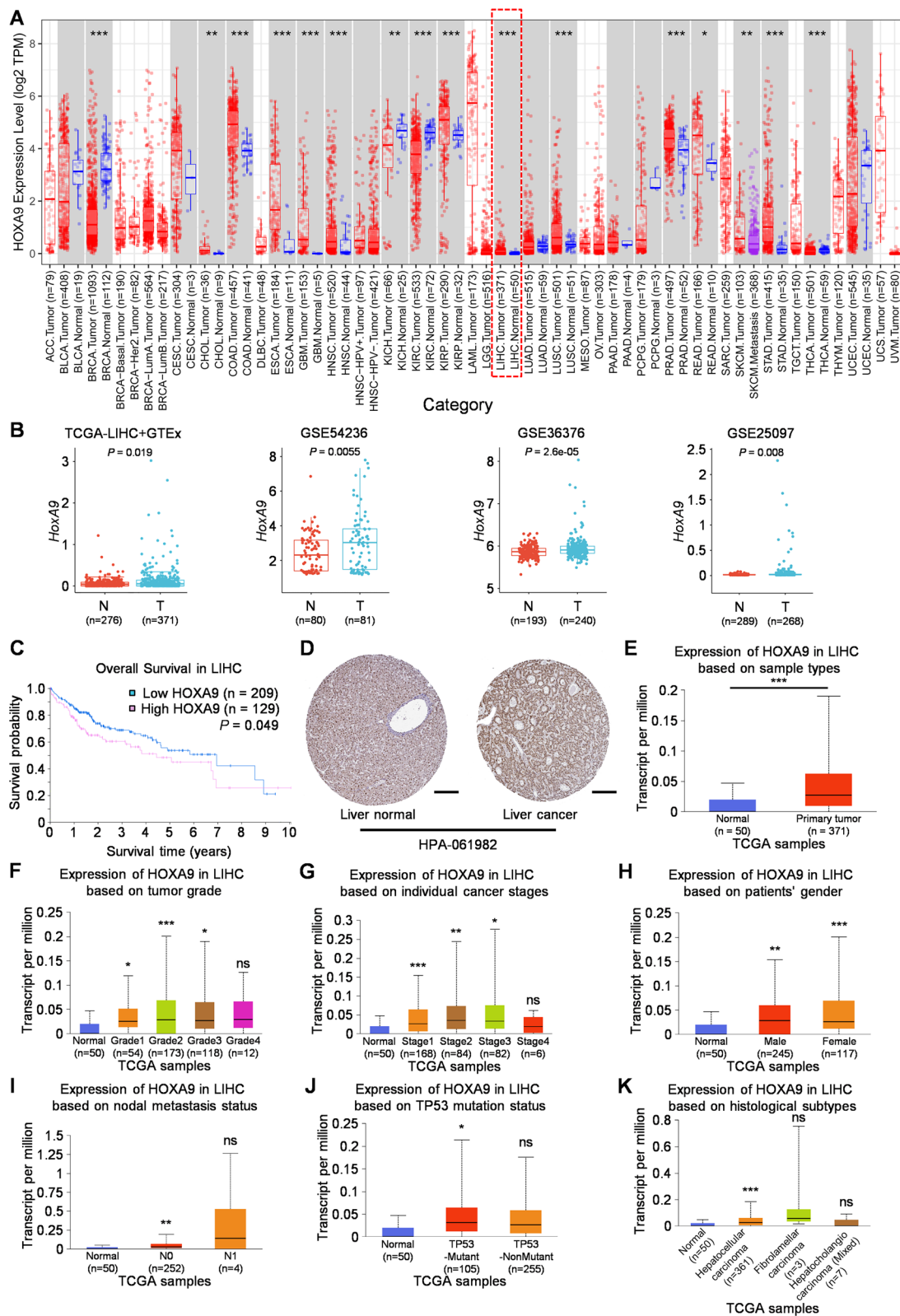
◄**Fig. 1** *HoxA9* RNA expression was significantly upregulated in HCC and upregulation of HOXA9 in HCC predicts poor prognosis. **A** TCGA datasets were used to analyze the RNA expression of *HoxA9* in tumors from TIMER2.0. The RNA expression of *HoxA9* was low in normal liver tissues and the expression of *HoxA9* was significantly upregulated in hepatocellular carcinoma (red virtual box); **B** The RNA expression of *HoxA9* was significantly upregulated in liver cancer tissues according to the TCGA+GTEx and multi-GEO datasets. The GEO liver cancer datasets include: GSE54236, GSE36376, GSE25097. **C** Kaplan–Meier curves of overall survival (OS) in HOXA9^{high} and HOXA9^{low} patients with LIHC using TCGA data from the HPA database; **D** the expression difference of HOXA9 at the protein level in liver tissues showed by immunohistochemical results from HPA public database (antibody number HPA-061982); Scale bars, 200 μm; **E–K** Box plots evaluating HOXA9 expression among different groups of patients based on clinical parameters in LIHC using the UALCAN database. Analysis is shown for sample types (**E**), tumor grades (**F**), cancer stage (**G**), sex (**H**), metastasis (**I**), TP53 mutation status (**J**) and histological subtypes (**K**). N0: no regional lymph node metastasis; N1: metastases in 1 to 3 axillary lymph nodes. All the datasets were collected from the Human Protein Atlas website (https://www.proteinatlas.org/) and the UALCAN database (http://ualcan.path.uab.edu/analysis-prot.html). ***$P < 0.001$, **$P < 0.01$, *$P < 0.05$

cells proportion scores with staining intensity scores. The proportion of positive cells score : 0, 0%; 1, ≤10%; 2, 11–50%; 3, 51–80%; and 4, ≥81%. The staining intensity score: 0, negative; 1, weak; 2, moderate; 3, strong.

Animals

Athymic male nude mice with the background of BALB/c-Nude (Gempharmatech, China) were purchased from germ free at 4 weeks old. All mice were provided with food and water AD libitum and maintained on a 12-hour light-dark cycle in a standard SPF-grade animal house at the Nanjing University (Nanjing, China). All animal experiments and experimental procedures were approved by the Ethics Committee of The First Affiliated Hospital of Anhui Medical University and also complied with the guidelines of the Guide for the Care and Use of Laboratory Animals prepared by the National Academy of Sciences and published by the National Institutes of Health (NIH Publication 86-23, revised 1985).

Xenograft tumor model in nude mice

To establish a subcutaneous xenograft model in athymic BALB/c nude mice, we injected 2,000,000 indicated HCC cells (Hep3B/MHCC-97H) into a single nude mouse to form a subcutaneous tumor and grow for 4 weeks, and measured the tumor diameter once each 7 days. Tumor volume (mm^3) was calculated with formula: $V = 0.5 \times Length \times Width^2$. Approximately four weeks after cell injection, mice were sacrificed and tumors were collected.

Statistical analysis

Data of bioinformatic analysis were downloaded and collated with R (Version 4.1.2, https://www.r-project.org) and RStudio (https://www.rstudio.com/). Unpaired, two-tailed Student's *t*-test was used for comparison between the two groups. Paired *t*-test was used to compare paired data. In other ways, Fisher's exact probability statistical analysis was chosen depending on the sample size and the size of the theoretical frequency. SPSS 24.0 software and GraphPad Prism 8 were used for statistical analysis and mapping. All functional experiments were repeated at least three times, and all data were expressed as mean ± standard deviation (SD). And *$P < 0.05$, **$P < 0.01$, and ***$P < 0.001$ were considered statistically significant.

Results

HOXA9 is dramatically upregulated in hepatocellular carcinoma

To explore the expression of *HoxA9* in different organ and tissues, we analyzed mouse single-cell transcriptome dataset (GSE109774) derived from Tabula Muris (Supplementary Figure 1A). The mRNA level of *HoxA9* gene was highly expressed in bladder, kidney, muscle and marrow, and rarely expressed in heart, aorta, liver, thymus, tongue, trachea, spleen, mammary gland, and lung (Supplementary Figure 1B, C).

HoxA9 gene has been found to be aberrant expressed in several solid tumors, including colon cancer, nasopharyngeal carcinoma and breast cancer (Bhatlekar et al. 2014). The analysis of expression profiles in 33 tumors of TCGA (The Cancer Genome Atlas) database showed that *HoxA9* mRNA was significantly upregulated in CHOL (cholangiocarcinoma), COAD (colon cancer), ESCA (Esophageal carcinoma),GBM (Glioblastoma multiforme), HNSC (head and neck squamous cell carcinoma), KIRP (Kidney renal papillary cell carcinoma), LIHC (hepatocellular carcinoma), LUSC (lung squamous cell carcinoma), PRAD (Prostate adenocarcinoma), READ (rectal cancer) and STAD (Stomach adenocarcinoma) and was significantly downregulated in BRCA (Breast invasive carcinoma), KICH (Kidney Chromophobe), KIRC (renal clear cell carcinoma), THCA (Thyroid carcinoma) (Figure 1A). These results are consistent with the previous studies that *HoxA9* gene plays opposite roles in the development of distinct cancers (Bhatlekar et al. 2014). Surprisingly, the mRNA level of *HoxA9* gene was upregulated in HCC tumors compared to adjacent non-tumor tissues, which was never reported before. Similar results were obtained by analyzing different HCC cohorts derived from TCGA+GTEx and Gene Expression Omnibus (GEO)

datasets (Figure 1B), implying a potential and important role of *HoxA9* in HCC development.

Upregulation of HOXA9 in HCC predicts poor prognosis

To investigate whether HOXA9 expression correlates with patients' survival, we analyzed it in HOXA9^{high} and HOXA9^{low} patients with liver cancer from the Human Protein Atlas (HPA) database. As expected, patients with HOXA9^{high} liver tumors had a worse median survival than HOXA9^{low} tumors (Figure 1C). In terms of protein expression levels in LIHC and normal tissues, immunohistochemistry results in HPA database showed that *HoxA9* was highly expressed in liver cancer (Figure 1D).

HOXA9 expression among groups of patients according to different clinical parameters in TCGA dataset demonstrated that a significant increase in HOXA9 expression was observed in sample types (Figure 1E), tumor grades (Figure 1F), tumor stages (Figure 1G), both sexes (Figure 1H), cancer stages (Figure 1I), TP53-mutant (Figure 1J), histological subtypes (Figure 1K) of LIHC patients compared to corresponding normal controls. These results suggest that HOXA9 is a prognostic indicator for the patients with liver cancer, which are highly aggressive and lethal.

HOXA9 expression in clinical HCC samples

To further confirm the upregulation of *HoxA9* gene in HCC tumors, both mRNA and protein levels of *HoxA9* were analyzed in 24 paired specimens of tumor and adjacent nontumor tissues. To verify the expression of HOXA9 in HCC tissues, we investigated the mRNA level of *HoxA9* in 12 pairs of tumor and adjacent non-tumor tissues by real-time PCR. Consistently, HOXA9 expression was significantly increased in HCC samples (Figure 2A, B). HOXA9 expression was also significantly increased in human HCC cell lines (HepG2, Hep3B, HCC-LM3, Huh7 and MHCC-97H) campared with normal human hepatocyte cell line (THLE-2) (Figure 2C, D). Then the expression of HOXA9 in tumor tissues and parallel non-tumor tissues resected from patients with HCC were assessed by IHC, which confirmed the protein level of HOXA9 in HCC was higher than that in adjacent tissues (Figure 2E). These results suggest that the expression of HOXA9 is upregulated in HCC.

HOXA9 promotes cell proliferation of HCC in vitro and in vivo

To explore the functions of HOXA9 in HCC tumorigenesis, we conducted overexpression and knockdown of HOXA9 in HCC cells. HCC cell lines were performed HOXA9 knockdown with lentivirus-based shRNA. On the other hand, we also transfected HOXA9 overexpressing plasmid (pLVX-Flag-HOXA9) into HCC cell lines (Figure 3A). Afterwards, CCK-8 and EdU assays demonstrated that knockdown of HOXA9 significantly inhibited cell proliferation in Hep3B and MHCC-97H cell lines (Figure 3B, C), which was consistent with the results of colony formation assays (Figure 3D). On the contrary, HOXA9 overexpressing in Hep3B and MHCC-97H cells significantly promoted cell proliferation (Figure 3B–D).

To investigate the effect of HOXA9 on HCC tumorigenesis in vivo, we delivered a xenograft tumor model in nude mice (Figure 3E). As observed, knockdown of HOXA9 significantly suppressed tumor growth and shHOXA9 groups gained lighter weights (Figure 3F) and smaller volumes (Figure 3G) in tumors formed from MHCC-97H cells. Besides, HOXA9 overexpressing groups showed opposite results in tumors formed from Hep3B cells. Overall, HOXA9 plays a promoting role in HCC proliferation both in vitro and in vivo.

HOXA9 propels HCC metastasis and prevents apoptosis in vitro

The wound healing and transwell assays of HCC cells confirmed that silencing of HOXA9 significantly weakened the cell migration ability in wound healing assay (Figure 4A) and migration and invasion cells in HOXA9 knockdown groups were fewer than that in the control group (Figure 4B). By contrast, overexpressing of HOXA9 showed an opposite trend. Overall, these results suggest that HOXA9 may play a promoting role in HCC metastasis in vitro.

Meanwhile, flow cytometric analysis in HCC cells confirmed that the apoptosis rates of shHOXA9 groups in HCC cells were significantly increased (Figure 4C). Besides, intended proteins were detected by Western blot analysis. Pro-apoptosis protein BAK was upregulated and anti-apoptosis protein BCL-2 was downregulated in shHOXA9 groups of HCC cells (Figure 4D). Meanwhile, a rise of protein levels of Caspase3 and Cleaved-Caspase3 was also observed in shHOXA9 groups (Figure 4D). By contrast, HOXA9 overexpressing groups showed opposite results. Thus, the data above suggested that HOXA9 prevents apoptosis in HCC cells.

HOXA9 expression is regulated by RPL38 in HCC

Ribosomal Protein L38 (RPL38) has been known to regulate Homeobox (*Hox*) genes' expression via IRES dependent translation (Kondrashov et al. 2011; Xue et al. 2014). To investigate whether RPL38 regulates HOXA9 expression in HCC, RPL38 was ablated in two human HCC cell lines (Hep3B and HCC-LM3) or overexpressed in human HCC cell line MHCC-97H (Figure 5A, B). Whereas RPL38
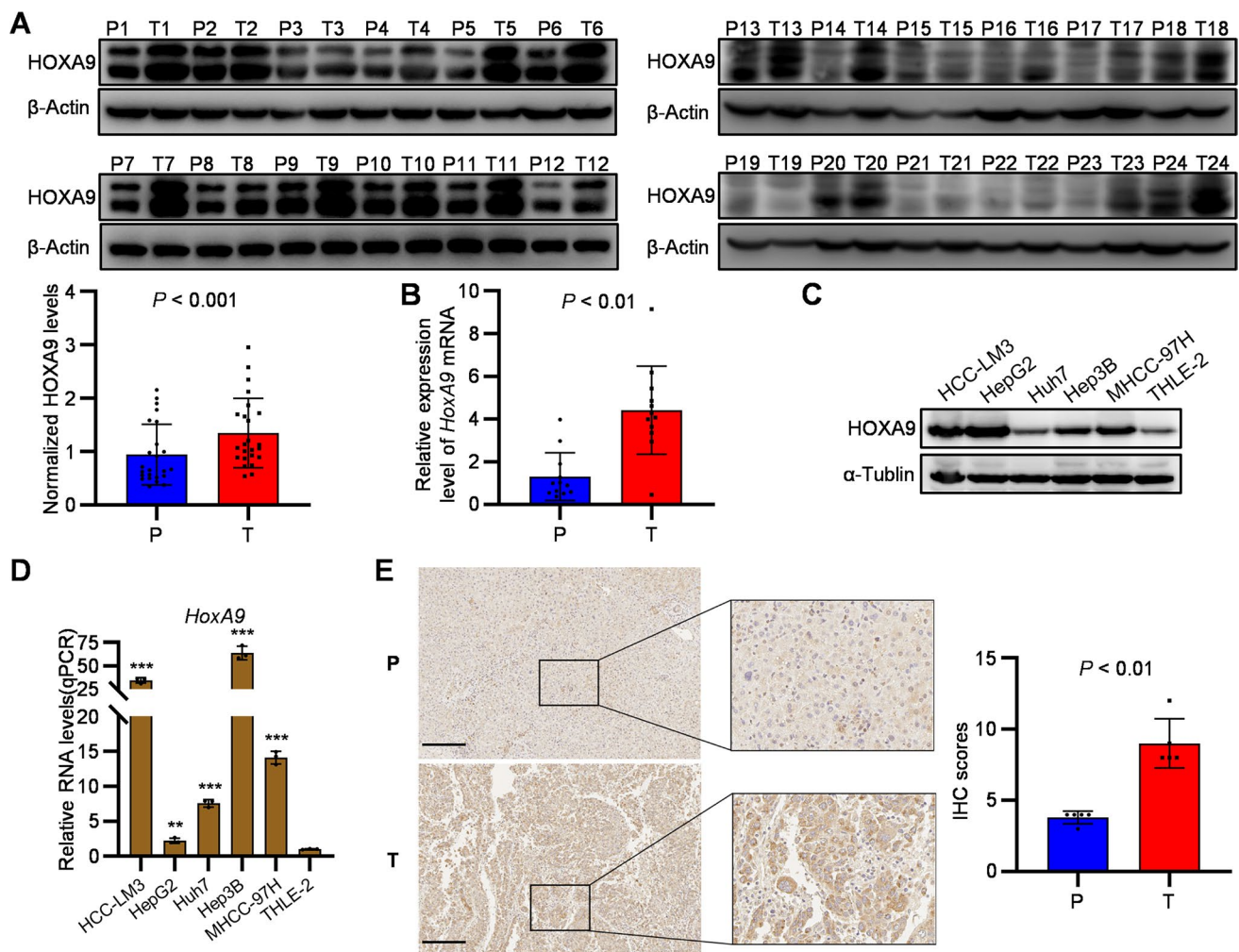
Fig. 2 HOXA9 promotes tumorigenesis in HCC samples and cell lines. **A** The expression levels of HOXA9 in tumor tissues (T) and paracancer tissues (P) of 24 HCC patients were compared by Western blot. ImageJ was used to calculate the gray value and compare the HOXA9 Fold for statistical analysis (HOXA9 Fold=HOXA9/β-Actin; $P<0.05$); The original blots are presented in Supplementary Fig. 4A; **B** The RNA expression of *HoxA9* in HCC tumor and adjacent non-tumor tissues was detected by qPCR; **C** Western blotting confirmed that HOXA9 was highly expressed in HCC cell lines compared with Human normal liver cell line THLE-2; The original blots are presented in Supplementary Fig. 4B; **D** The RNA expression of *HoxA9* in HCC cell lines compared with Human normal liver cell line THLE-2 was detected by qPCR. **E** Immunohistochemical staining and statistical analysis of HOXA9 in paired cancer tissues (T) and paracancer tissues (P) from (number) HCC patients. Scale bars, 200 μm; Results are means±SD (n=5 per group); ***$P<0.001$, **$P<0.01$, *$P<0.05$. Statistical analysis was determined by Student's t-test

ablation decreases the protein level of HOXA9, overexpression of RPL38 increases it (Figure 5A, B). Curiously, the mRNA level of HOXA9 was also regulated by RPL38 whose expression positively correlated with HOXA9 mRNA level (Figure 5C). Taken together, these results suggest that both mRNA and protein levels of HOXA9 were controlled by RPL38.

Meanwhile, RNA-sequencing was conducted in parental and RPL38-ablated HCC-LM3 cells. Intriguingly, the mRNA levels of multiple *Hox* genes were dramatically upregulated or downregulated by RPL38 ablation (Figure 5D). qRT-PCR analysis of several *Hox* genes in human cancer cell lines or normal human hepatocytes showed that while RPL38 expression positively correlated with the mRNA levels of HOXA7, HOXA10, and HOXA13 genes (Figure 5E, F), it has a reversed effect on the expression of HOXA1, HOXA2 and HOXA5 genes (Figure 5G, H). These results suggest that in addition to upregulation of HOXA9 expression, RPL38 displays opposite effects on distinct *Hox* genes' expression.

Identification of HOXA9-interacting genes and proteins analysis

To better explore the underlying pathogenic mechanism of HOXA9 in LIHC, the coexpressed genes of HOXA9 were
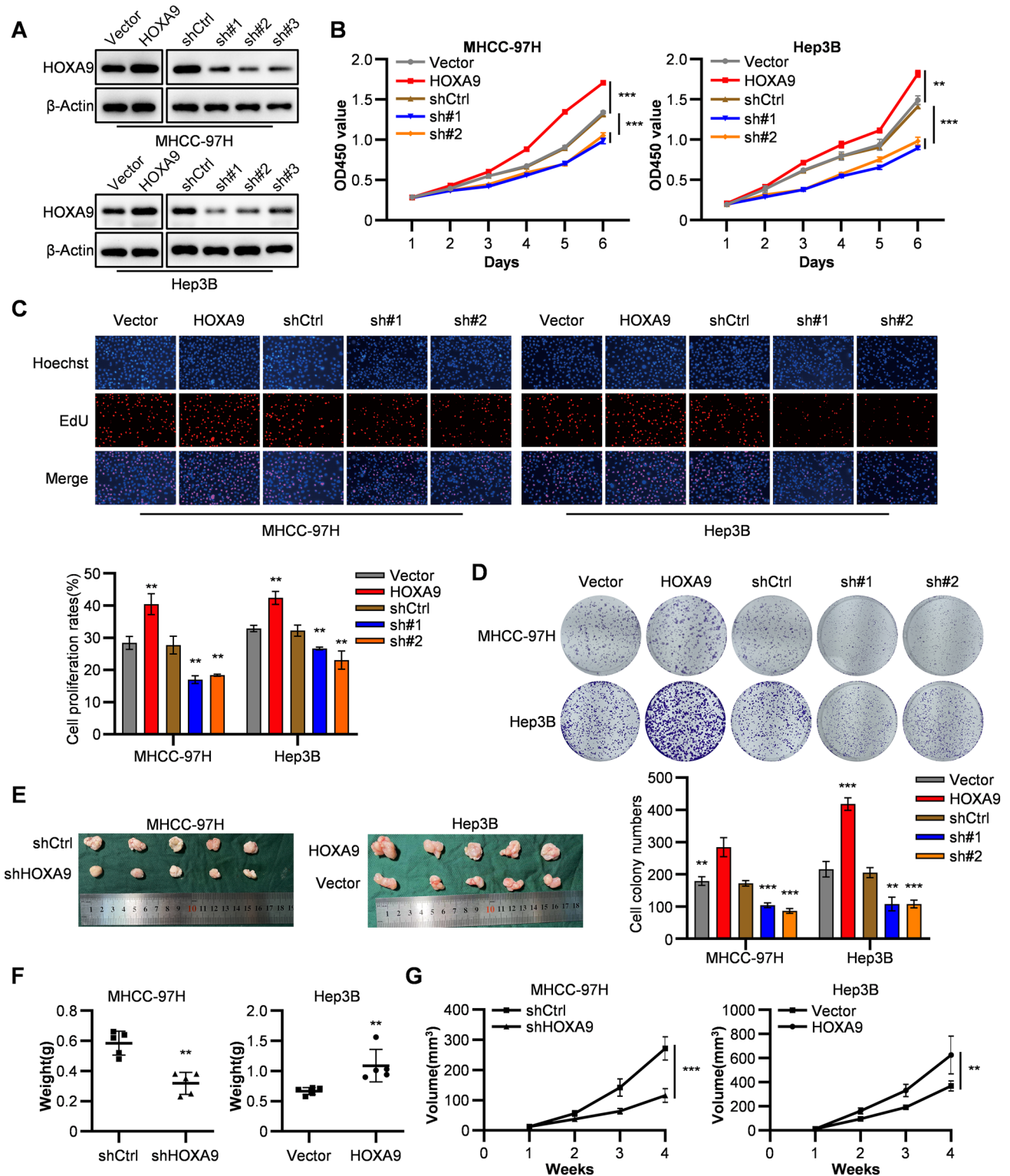
screened out in TCGA-LIHC patients using the LinkedOmics database (Figure 6A). The top 50 genes that were positively and negatively correlated with HOXA9 in LIHC are shown (Figure 6B, C).

Notably, in terms of cellular composition (CC), and molecular function (MF), HOXA9 was enriched in DNA methylation processes, such as methyltransferase complex and methyl-CpG binding in LIHC (Figure 6D). In addition, the top 10 KEGG pathways for HOXA9 and its correlated

◄**Fig. 3** HOXA9 promotes proliferation in HCC cell lines. **A** The efficiency of transfection of HOXA9 knockdown and overexpressing were detected by western blot. The original blots are presented in Supplementary Fig. 4C. **B–C** CCK8 assays (**B**) and EdU asseys (**C**) were performed to measure cell proliferation ability of HOXA9 overexpression and shRNA knockdown groups in MHCC-97H and Hep3B cells compared with the control groups. Data are shown as means ± SD (n = 3). **D** Colony formation assays were performed to measure cell proliferation ability of HOXA9 overexpression and shRNA knockdown groups in MHCC-97H and Hep3B cells compared with the control groups. Data are shown as means ± SD (n = 3). **E** Images of nude mice with tumors formed from MHCC-97H cells with shRNA knockdown and Hep3B cells with HOXA9 overexpression groups compared with the control groups. **F** The weight of tumor samples in each group formed from MHCC-97H and Hep3B cells mentioned above by the time of harvest. **G** The tumor growth curves were measured after the injection of MHCC-97H and Hep3B cells in each group once the tumor had formed, and the volume was calculated every 7 days. Data are shown as means ± SD (n = 5 per group); ***$P < 0.001$, **$P < 0.01$, *$P < 0.05$. Statistical analysis was determined by Student's *t*-test

genes are shown in Figure 6E. Among these pathways, some immune-related pathways were highly associated with HOXA9, including T cell receptor signaling pathway, Th1 and Th2 cell differentiation and Natural killer cell mediated cytotoxicity in LIHC (Figure 6E). These results strongly imply that HOXA9 is involved in the regulation of DNA methylation and immune infiltration in liver cancer.

Correlations between HOXA9 and immune cell infiltration in the tumor microenvironment (TME)

The tumor microenvironment (TME) plays a critical role in the development and progression of HCC. Studies indicate that HCC employs multiple immunomodulatory mechanisms to disrupt the immune system (Flecken et al. 2012). We further explored the correlations between HOXA9 expression and immune cells in the TME that HOXA9 expression presented strong connections to CD4+ T cells, CD8+ T cells, neutrophils, macrophages and dendritic cells (DCs) in LIHC (Supplementary Figure 2A). Then, a heatmap showed correlation between HOXA9 expression and the above 6 immune cells in TME of TCGA-LIHC dataset (Supplementary Figure 2B). Besides, there was a statistically significant positive correlation between HOXA9 expression and the immune infiltration levels of three types of immune cells: CD4+ T cells (R = 0.21, P = 8.2e-5), neutrophils (R = 0.18, P = 4.0e−4) and macrophages (R = 0.55, P = 0.03) for LIHC cases (Supplementary Figure 2C). These results showed close correlations between HOXA9 and immune cell infiltration in the tumor microenvironment (TME).

To deepen our understanding of HOXA9 with the immune response, we validated the correlations between HOXA9 expression and diverse immune signatures in LIHC. After adjusting for tumor purity, HOXA9 expression was significantly associated with most immune markers of immune cells in LIHC (Supplementary Table 3). We also examined the correlation between HOXA9 expression and various functional T cells and HOXA9 expression was significantly correlated with 32 of 38 T-cell markers in LIHC after adjusting for tumor purity (Supplementary Table 4). These findings further support that HOXA9 expression is significantly related to immune infiltration and HOXA9 might be vital in regulating immune cell infiltration.

DNA methylation analysis of HoxA9 gene

The validation of the DNA methylation status from TCGA data showed that the promoter methylation level of HOXA9 was significantly elevated in LIHC tissues of patients in terms of sample types, tumor grades, tumor stages, both sexes, cancer stages, TP53-mutant and TP53 wild-type LIHC patients compared to normal controls (Supplementary Figure 3A–F). To summary, these results suggest that DNA methylation of HOXA9 may be a potienal prognostic indicator for LIHC patients.

Discussion

Years of studies have suggested that HOXA9 is involved in a variety of solid cancers, including Colon carcinoma, Breast cancer and Glioblastoma (Bhatlekar et al. 2014). Although many studies have shown that *Hox*A9 affects cancer development, the role of *HoxA9* gene in HCC development haven't been investigated before. Here we found HOXA9 was highly expressed in HCC patients, which predicted poor prognosis.

Recent studies have found that tumor-infiltrating immune cells cause T cell dysfunction to promote the escape of cancer cells from the T cell phenotypic immune system, leading to tumor invasion and metastasis (Liu et al. 2022). According to our analysis, the expression of HOXA9 in liver cancer is positively correlated with immune T cell infiltration, suggesting that HOXA9 could approximately lead to tumor metastasis by weakening the function of T cells. Therefore, clinical treatment targeting HOXA9 may be a potential direction for anti-liver cancer immunotherapy.

HOXA9 promoter methylation is common in oral cancer, whose level is higher in tumor with a higher risk of metastasis (Uchida et al. 2014). In addition, HOXA9 and ISL1 methylation can be used to predict prognosis in patients with high-grade non-invasive bladder cancer (Kitchen et al. 2015). Considering HOXA9 and methylation-related genes among our findings, further experiments can be conducted to verify their interactions and promoting mechanisms for HCC development. A typical study was conducted to detect abnormal methylation of HOXA9 and HIC1 in serum DNA for early diagnosis of epithelial ovarian cancer, suggesting
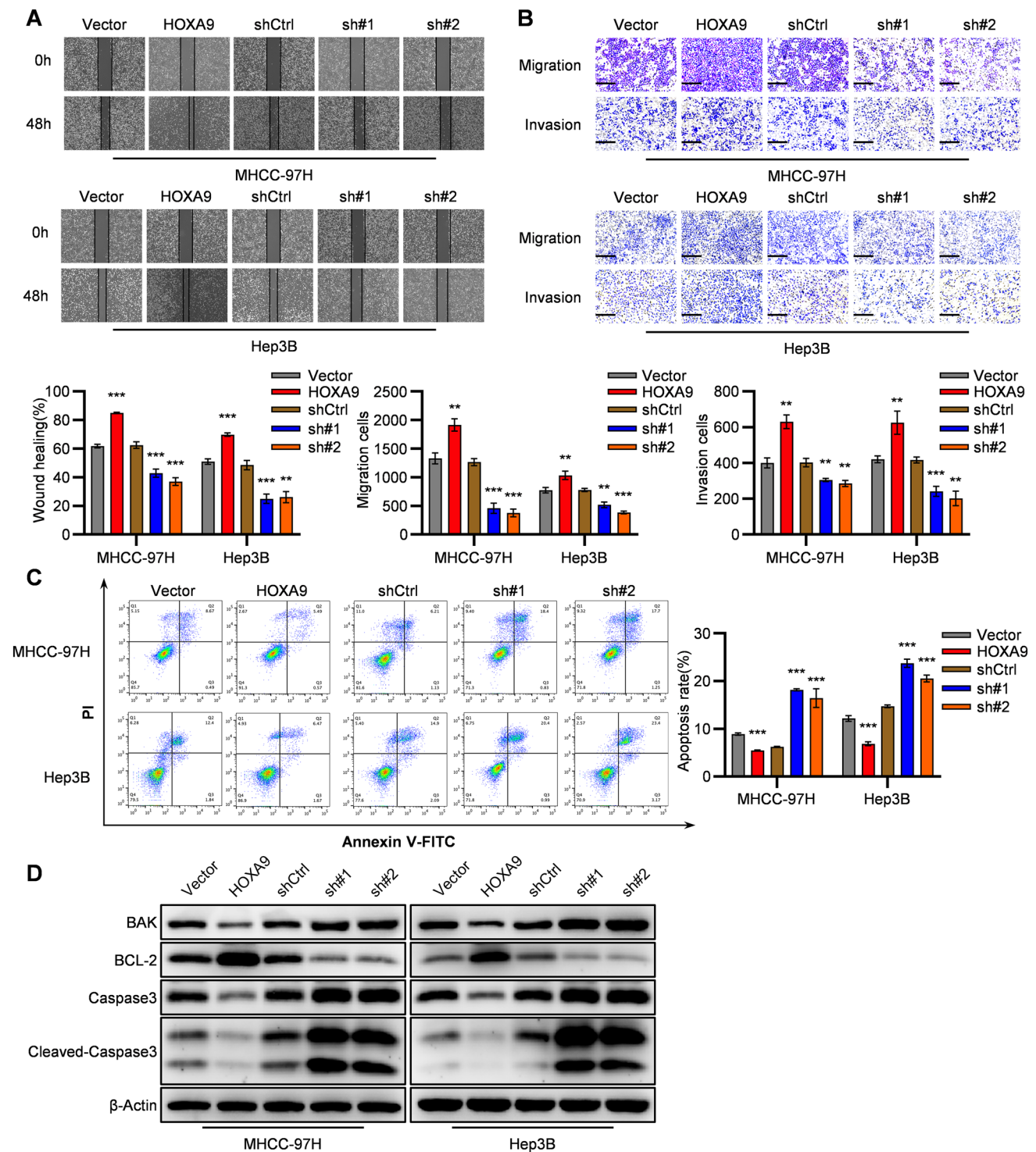
Fig. 4 HOXA9 promotes migration, invasion and prevents apoptosis in HCC cell lines. **A–B** Representative images and quantification of the effect of HOXA9 overexpression and shRNA knockdown groups on cell migration or invasion through wound healing assay (**A**) and transwell assay (**B**) in MHCC-97H and Hep3B cells compared with the control group. Scale bar, 200 μm. Results are means ± SD (n = 3 per group); **C** Flow cytometry analysis was performed to measure cell apoptosis rates of HOXA9 overexpression and shRNA knockdown groups in MHCC-97H and Hep3B cells compared with the control group. Data are shown as means ± SD (n = 3); **D** The BAK, BCL-2, Caspase3, Cleaved-Caspase3 and β-Actin were detected by Western blot analysis in HOXA9 knockdown and overexpressing HCC cells (Hep3B and MHCC-97H). The original blots are presented in Supplementary Fig. 4D; ***P < 0.001, **P < 0.01, *P < 0.05. Statistical analysis was determined by Student's t-test
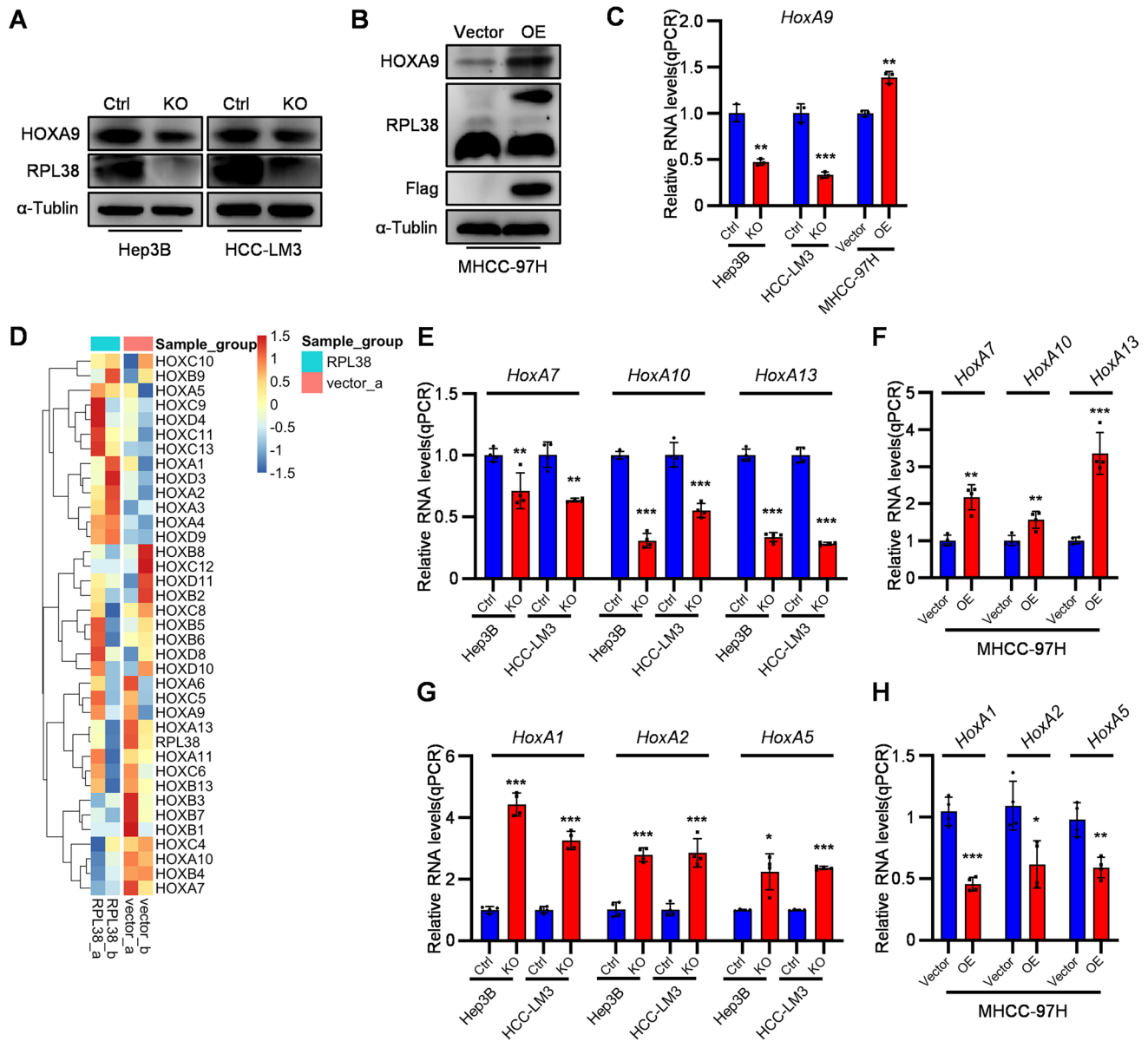
Fig. 5 RPL38 regulates the expression of several Homeobox genes, including *HoxA9*. **A** HCC cell lines (Hep3B and HCC-LM3) were performed RPL38 knockout with CRISPR/Cas9 plasmids compared with the control groups. The HOXA9, RPL38 and α-Tublin were detected by Western blot analysis in RPL38-silenced HCC cells (Hep3B and HCC-LM3). The original blots are presented in Supplementary Fig. 4E; **B** MHCC-97H cell line was transfected with the RPL38 overexpressing plasmid (pLVX-Flag-RPL38) compared with the control group. The HOXA9, RPL38 and α-Tublin were detected by Western blot analysis in MHCC-97H RPL38-overexpressing cell line. The original blots are presented in Supplementary Fig. 4E; **C** The RNA expression of *HoxA9* in RPL38-silenced Hep3B and HCC-LM3 cells and MHCC-97H RPL38-overexpressing cell line were detected by qPCR; Data are shown as means ± SD (n = 3); **D** Hierarchical clustering analysis of differentially expressed genes between RPL38-silenced (Cas9-RPL38 knockout) and control of HCC-LM3 cells. A heat map of selected Homeobox genes with significant differences was made; **E** The RNA expression of *HoxA7*, *HoxA10*, *HoxA13* in RPL38-silenced Hep3B and HCC-LM3 cells were detected by qPCR; Data are shown as means ± SD (n = 4); **F** The RNA expression of *HoxA7*, *HoxA10*, *HoxA13* in MHCC-97H RPL38-overexpressing cell line were detected by qPCR; Data are shown as means ± SD (n = 4); **G** The RNA expression of *HoxA1*, *HoxA2*, *HoxA5* in RPL38-silenced Hep3B and HCC-LM3 cells were detected by qPCR; Data are shown as means ± SD (n = 4); **H** The RNA expression of *HoxA1*, *HoxA2*, *HoxA5* in MHCC-97H RPL38-overexpressing cell line were detected by qPCR; Data are shown as means ± SD (n = 4); ***$P < 0.001$, **$P < 0.01$, *$P < 0.05$. Statistical analysis was determined by Student's *t*-test
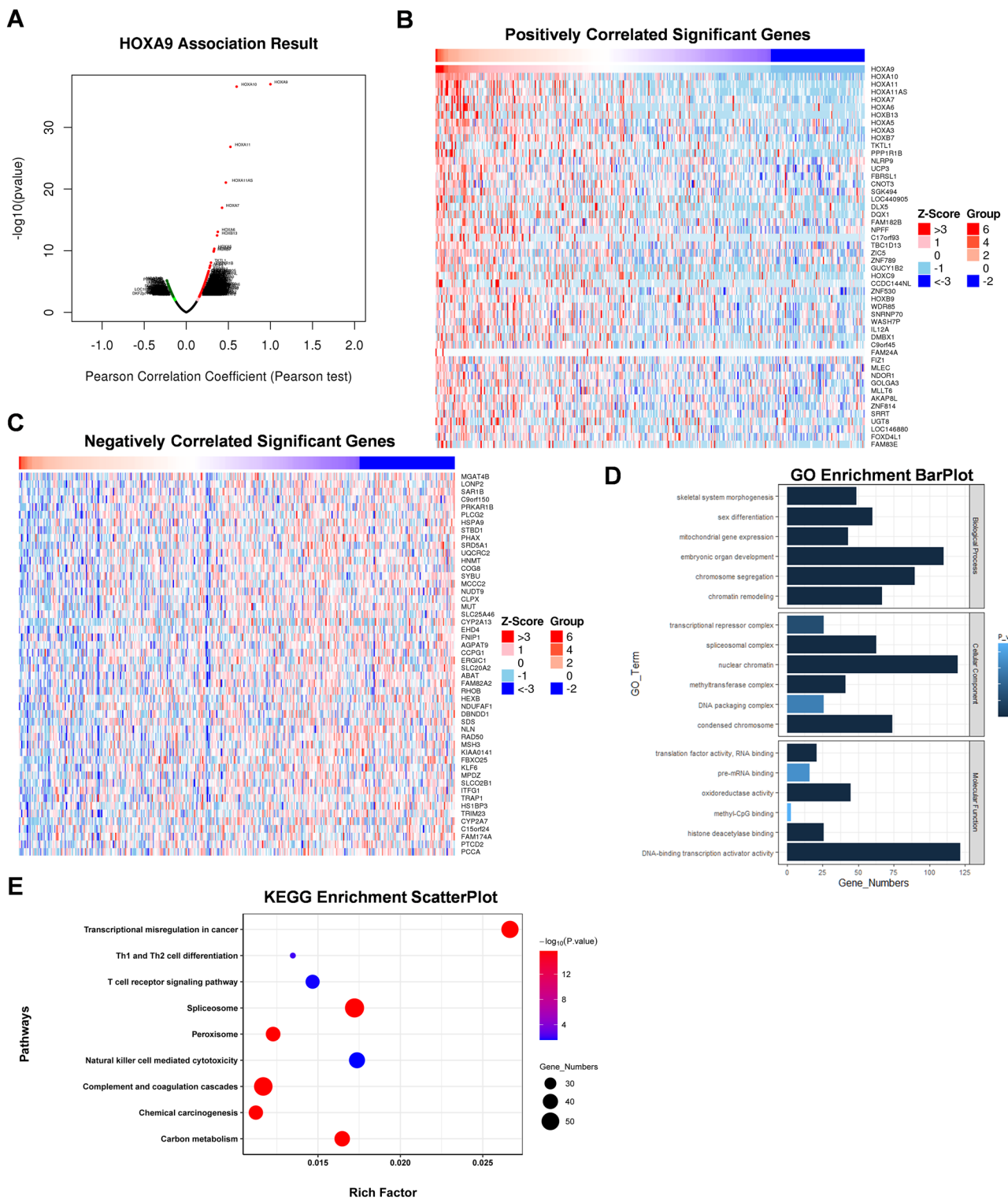
Fig. 6 HOXA9-related genes and enrichment analysis. **A** Coexpressed genes associated with HOXA9 in HCC, analyzed by using LinkedOmics and visualized by Volcano plot; **B** Heat maps showing the top 50 genes positively correlated with HOXA9 in HCC; **C** Heat maps showing the top 50 genes negatively correlated with HOXA9 in HCC; **D** GO enrichment analysis of genes correlated with HOXA9, including biological process, cellular component and molecular functions; **E** KEGG enrichment analysis of top genes correlated with HOXA9

whether HOXA9 methylation detection in serum DNA can be applied in the diagnosis of HCC, which is more clinically valuable (Singh et al. 2020).

In addition, we speculated HOXA9 may also be regulated by ribosomal protein RPL38 in liver cancer cells in addition to bone development of mouse embryo from previous reports (Kondrashov et al. 2011). We found that knockout of RPL38 significantly reduced both the RNA and protein levels of *HoxA9* in HCC cells. However, it is worth noting that the genes of the Homeobox family are inconsistently affected by the regulation of ribosomal protein RPL38, showing different changes at RNA levels, which may be interesting for further investigation. Besides, HOXA9 expression was either upregulated or downregulated in other cancers, implying a complexed role of HOXA9 in the development of different cancers, which may be caused by the distinct levels of RPL38 whose expression dictated protein and mRNA levels of *HoxA9*. Although studies have shown that RPL38 can identify IRES domains specifically to adjust the mRNA translation, there were no measurements of genome-wide translation to exclude other complex mechanisms, such as altered synthesis of other proteins (Kondrashov et al. 2011; Xue et al. 2014). Thus, how RPL38 directly or indirectly regulate *Hox* genes transcription in addition to its mRNA translation need to be further investigated.

This study adds to our understanding of HOXA9 and liver cancer, but limitations remain. Firstly, although we have investigated the relationship between HOXA9 and immune infiltration in HCC patients, there is currently a lack of interpretation based on immunoassays of different subpopulations and validation from clinical trials. Secondly, the relationships between the mechanism of immune infiltration of HOXA9 and the role of HOXA9 in tumor growth, metastasis, and apoptosis remains further exploration. Lastly, we preliminarily confirm that HOXA9 is closely related to the immune microenvironment in HCC, but there is no direct evidence to prove the effect of HOXA9 on immunotherapy efficacy and prognosis. More future studies are needed to confirm the prognostic and immunological value of HOXA9 and its underlying mechanisms.

Conclusion

Supplementary Information The online version contains supplementary material available at https://doi.org/10.1007/s00432-024-05950-9.

Declarations

References

Bhatlekar S, Fields JZ, Boman BM (2014) HOX genes and their role in the development of human cancers. J Mol Med (Berl) 92(8):811–823. https://doi.org/10.1007/s00109-014-1181-y

Collins CT, Hess JL (2016) Deregulation of the HOXA9/MEIS1 axis in acute leukemia. Curr Opin Hematol 23(4):354–361. https://doi.org/10.1097/moh.0000000000000245

Donne R, Lujambio A (2023) The liver cancer immune microenvironment: therapeutic implications for hepatocellular carcinoma. Hepatology 77(5):1773–1796. https://doi.org/10.1002/hep.32740

Fitzmaurice C, Akinyemiju TF, Al Lami FH, Alam T, Alizadeh-Navaei R, Naghavi M, Global Burden of Disease Cancer, Collaboration (2018) Global, regional, and national cancer incidence, mortality, years of life lost, years lived with disability, and disability-adjusted life-years for 29 cancer groups, 1990 to 2016: a systematic analysis for the global burden of disease study. JAMA Oncol 4(11):1553–1568. https://doi.org/10.1001/jamaoncol.2018.2706

Flecken T, Spangenberg HC, Thimme R (2012) Immunobiology of hepatocellular carcinoma. Langenbecks Arch Surg 397(5):673–680. https://doi.org/10.1007/s00423-011-0783-x

Gilbert PM, Mouw JK, Unger MA, Lakins JN, Gbegnon MK, Clemmer VB, Weaver VM (2010) HOXA9 regulates BRCA1 expression to modulate human breast tumor phenotype. J Clin Invest 120(5):1535–1550. https://doi.org/10.1172/jci39534

Kitchen MO, Bryan RT, Haworth KE, Emes RD, Luscombe C, Gommersall L, Farrell WE (2015) Methylation of HOXA9 and ISL1 predicts patient outcome in high-grade non-invasive bladder cancer. PLoS ONE 10(9):e0137003. https://doi.org/10.1371/journal.pone.0137003

Kondrashov N, Pusic A, Stumpf CR, Shimizu K, Hsieh AC, Xue S, Barna M (2011) Ribosome-mediated specificity in Hox mRNA translation and vertebrate tissue patterning. Cell 145(3):383–397. https://doi.org/10.1016/j.cell.2011.03.028

Krumlauf R (2018) Hox genes, clusters and collinearity. Int J Dev Biol 62(11–12):659–663. https://doi.org/10.1387/ijdb.180330rr

Li L, Wang H (2016) Heterogeneity of liver cancer and personalized therapy. Cancer Lett 379(2):191–197. https://doi.org/10.1016/j.canlet.2015.07.018

Liu Y, Zhang Q, Xing B, Luo N, Gao R, Yu K, Zhang Z (2022) Immune phenotypic linkage between colorectal cancer and liver metastasis. Cancer Cell 40(4):424-437.e425. https://doi.org/10.1016/j.ccell.2022.02.013

Rumgay H, Arnold M, Ferlay J, Lesi O, Cabasag CJ, Vignat J, Soerjomataram I (2022) Global burden of primary liver cancer in 2020 and predictions to 2040. J Hepatol. https://doi.org/10.1016/j.jhep.2022.08.021

Singh A, Gupta S, Badarukhiya JA, Sachan M (2020) Detection of aberrant methylation of HOXA9 and HIC1 through multiplex MethyLight assay in serum DNA for the early detection of epithelial ovarian cancer. Int J Cancer 147(6):1740–1752. https://doi.org/10.1002/ijc.32984

Sung H, Ferlay J, Siegel RL, Laversanne M, Soerjomataram I, Jemal A, Bray F (2021) Global cancer statistics 2020: GLOBOCAN estimates of incidence and mortality worldwide for 36 cancers in 185 countries. CA Cancer J Clin 71(3):209–249. https://doi.org/10.3322/caac.21660

Tang L, Peng L, Tan C, Liu H, Chen P, Wang H (2022) Role of HOXA9 in solid tumors: mechanistic insights and therapeutic potential. Cancer Cell Int 22(1):349. https://doi.org/10.1186/s12935-022-02767-9

Uchida K, Veeramachaneni R, Huey B, Bhattacharya A, Schmidt BL, Albertson DG (2014) Investigation of HOXA9 promoter methylation as a biomarker to distinguish oral cancer patients at low risk of neck metastasis. BMC Cancer 14:353. https://doi.org/10.1186/1471-2407-14-353

Wu J, Yang S, Xu K, Ding C, Zhou Y, Fu X, Li L (2018) Patterns and trends of liver cancer incidence rates in eastern and southeastern Asian countries (1983–2007) and predictions to 2030. Gastroenterology 154(6):1719-1728 e1715. https://doi.org/10.1053/j.gastro.2018.01.033

Xu LX, He MH, Dai ZH, Yu J, Wang JG, Li XC, Kuang M (2019) Genomic and transcriptional heterogeneity of multifocal hepatocellular carcinoma. Ann Oncol 30(6):990–997. https://doi.org/10.1093/annonc/mdz103

Xue S, Tian S, Fujii K, Kladwang W, Das R, Barna M (2014) RNA regulons in Hox 5′ UTRs confer ribosome specificity to gene regulation. Nature 517(7532):33–38. https://doi.org/10.1038/nature14010

Zhou L, Wang Y, Zhou M, Zhang Y, Wang P, Li X, Ding Z (2018) HOXA9 inhibits HIF-1alpha-mediated glycolysis through interacting with CRIP2 to repress cutaneous squamous cell carcinoma development. Nat Commun 9(1):1480. https://doi.org/10.1038/s41467-018-03914-5